Journal of Hydrology 588 (2020) 124855

Contents lists available at ScienceDirect

Journal of Hydrology

journal homepage: www.elsevier.com/locate/jhydrol

Research papers

Pavement alters delivery of sediment and fallout radionuclides to urban streams

Allen C. Gellis[a,*], Christopher C. Fuller[b], Peter C. Van Metre[c], Barbara J. Mahler[c], Claire Welty[d,e], Andrew J. Miller[d,f], Lucas A. Nibert[g], Zach J. Clifton[a], Jeremy J. Malen[a], John T. Kemper[h]

[a] U.S. Geological Survey, Baltimore, MD, United States
[b] U.S. Geological Survey, Menlo Park, CA, United States
[c] U.S. Geological Survey, Austin, TX, United States
[d] Center for Urban Environmental Research and Education, University of Maryland, Baltimore County, Baltimore, MD, United States
[e] Department of Chemical, Biochemical, and Environmental Engineering, University of Maryland, Baltimore County, Baltimore, MD, United States
[f] Department of Geography and Environmental Systems, University of Maryland, Baltimore County, Baltimore, MD, United States
[g] Department of Geological Sciences, University of Alabama, Tuscaloosa, AL, United States
[h] Warner College of Natural Resources, Colorado State University, Fort Collins, CO, United States

Keywords:
Fallout radionuclides
Sediment
Urban
Buried channels

ARTICLE INFO

This manuscript was handled, with the assistance of Jian Luo, Associate Editor

ABSTRACT

Sediment from urban impervious surfaces has the potential to be an important vector for contaminants, particularly where stormwater culverts and other buried channels draining large impervious areas exit from underground pipes into open channels. To better understand urban sediment sources and their relation to fallout radionuclides, we collected samples of rainfall, urban sediment (pavement sediment, topsoil), streambank sediment, and fluvial sediment (suspended sediment and bed sediment) for ^{7}Be, $^{210}Pb_{ex}$, and ^{137}Cs analysis. The results indicate that each rainfall event tags pavement sediment with elevated activities of ^{7}Be and $^{210}Pb_{ex}$ such that runoff from impervious surfaces in the buried channel part of the stream network contains the highest activities. Pavement sediment, because it is characteristically a thin veneer, has a small mass to rainwater ratio resulting in a greater tagging of ^{7}Be and $^{210}Pb_{ex}$ activity than does topsoil on a per gram basis. An unmixing model indicated that suspended-sediment samples collected at the culvert outlet from the buried-channel network are from pavement sediment sources (45 ± 25%) with a smaller component of topsoil (22 ± 19%), and a component from streambanks (32 ± 35%) that we infer to be older channel material and subsoil eroded from within the culvert system. Downstream from the culvert, suspended sediment collected from the open-channel parts of the stream had ^{7}Be and $^{210}Pb_{ex}$ activities that were substantially reduced by the contribution of sediment from streambanks (57 ± 15%), with pavement contributions decreasing to 15 (±9%) and topsoil contributing 28 (±7%). The results highlight the utility of ^{7}Be, $^{210}Pb_{ex}$, and ^{137}Cs as tracers of urban sediment sources, resulting in a unique radionuclide signature for urban watersheds compared to other sediment-source settings.

1. Introduction

Many common urban contaminants, such as metals and polycyclic aromatic hydrocarbons (PAHs), sorb to sediment and are transported to streams with runoff (Sartor et al., 1974; Paul and Meyer, 2001; Mahler et al., 2005), yet sources of sediment to urban streams have not been well quantified. The three major sources of urban sediment—impervious-surface sediment, upland soils, and streambanks—are associated with different types and concentrations of contaminants. Impervious surface sediment can have high concentrations of contaminants from atmospheric deposition (e.g., Hg, PAHs) (Callender and Rice, 2000; Van Metre and Mahler, 2003;

* Corresponding author.
E-mail address: agellis@usgs.gov (A.C. Gellis).

https://doi.org/10.1016/j.jhydrol.2020.124855
Received 20 August 2019; Received in revised form 14 January 2020; Accepted 13 March 2020
Available online 16 March 2020
0022-1694/ Published by Elsevier B.V.

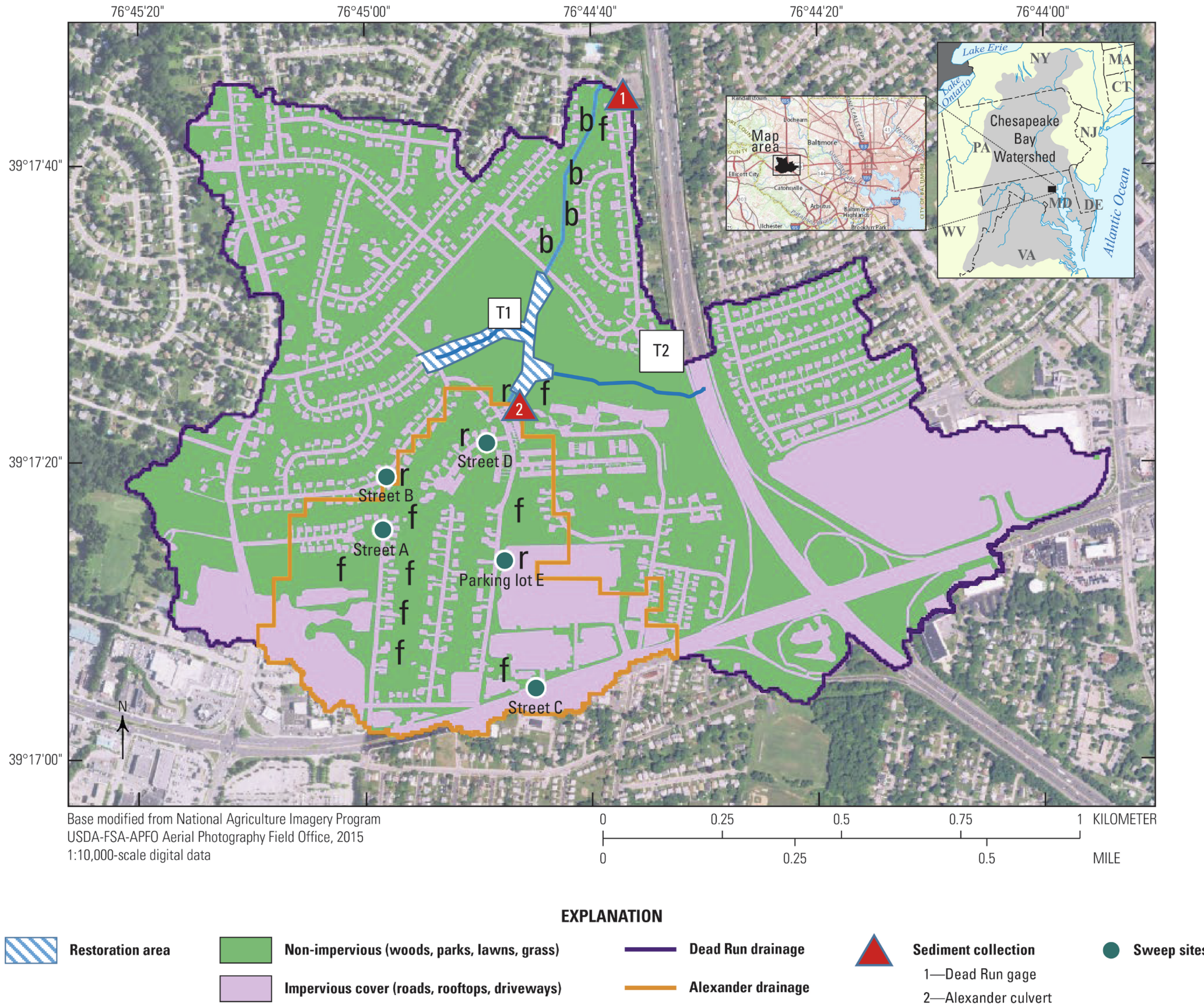

Fig. 1. Map of the Dead Run study area showing pavement sweep sites (Streets A-D, Parking Lot E),runoff samples, soil samples, and bank samples and tributaries (T1,T2) entering between the sediment collection sites Alexander Culvert (#2) and the Dead Run Gage (#1). [r = runoff sample, collection, f = soil sample collection, b = bank sample collection]

Boonyatumanond et al., 2007; Eckley and Branfireun, 2008; Thapalia et al., 2010), and wear of solid materials (e.g. roofing materials, pavement sealants, and galvanized metal) (Van Metre and Mahler, 2003; Mahler et al., 2005). Upland soils can contain pesticides and other products used in home and commercial outdoor applications as well as contaminants associated with urban non-point sources, legacy industrial sources, and atmospheric deposition (Cannon and Horton 2009; Hatcher and Filippelli 2010; Jorgenson and Young 2010; Watts et al. 2010, Bain et al., 2012). Streambanks are assumed to have negligible concentrations of anthropogenic contaminants, except perhaps in older developed parts of the United States where some streambanks contain legacy contamination from sediment deposited in the past (18th–19th centuries) (Southworth et al., 2013; Taylor and Owens, 2009).

It is well documented that urbanization and increased impervious cover leads to more runoff and higher peak flows (Leopold 1968; Paul and Meyer, 2001 Walsh et al., 2005). These hydrologic changes increase streampower, leading to channel widening, streambank erosion, and channel incision (Booth, 1990, 1991; Gellis et al., 2017a; Wolman, 1967). Thus, streambanks in urban environments are expected to contribute a large part of the total sediment load (Devereux et al., 2010; Gellis et al., 2017a; Cashman et al., 2018). In many urban areas, however, stream channels are paved over or buried during urbanization and directed into culverts, pipes, and concrete-lined ditches (Elmore and Kaushal, 2008; Napieralski and Carvalhaes, 2016). In these buried-channel parts of the watershed, streambank erosion does not occur and surface-derived sediment (e.g. soil, impervious surfaces) might be expected to dominate fluvial sediment (suspended sediment (SS) and bed sediment).

Radionuclides in atmospheric fallout—fallout radionuclides ^{7}Be, ^{210}Pb$_{ex}$ (excess ^{210}Pb, the part not supported by decay of parent radionuclides in geologic materials), and ^{137}Cs—are delivered to the Earth's surface primarily by rainfall and become a marker of surface-derived sediment. Eroding streambanks typically contain lower activities of ^{7}Be, ^{210}Pb$_{ex}$, and ^{137}Cs, because the vertical position of streambanks leads to little direct contact with rainfall (Matisoff et al., 2005; Hancock et al., 2014). Differences in ^{7}Be, ^{210}Pb$_{ex}$, and ^{137}Cs activities between geomorphic features (streambanks and upland surfaces) have been used to discriminate sediment sources and estimate the transport and transit times of sediment (Dominik et al., 1987; Evrard et al., 2010; Gellis et al., 2017b; Huon et al., 2017; Mabit et al., 2014; Matisoff et al., 2005; Olley et al., 2013a,b; Slimane et al., 2016; Froger et al., 2018; Wallbrink et al., 2002). Of these, only Froger et al. (2018) examined ^{7}Be, ^{210}Pb$_{ex}$, and ^{137}Cs activities and sediment processes in urban settings.

In an analysis of fluvial sediment for wadeable streams in the Midwest U.S., Gellis et al. (2017b) reported that stream sediment in watersheds with urban areas had higher activities of ^{7}Be and ^{210}Pb$_{ex}$ than stream sediment in agricultural and undeveloped settings (Supporting Information (Fig. S1). That study, however, considered only surface (agricultural) soil and streambank and channel erosion as endmember sources of stream sediment and did not differentiate sediment delivered from impervious surfaces in source partitioning. Froger et al. (2018) reported high ^{7}Be and ^{210}Pb$_{ex}$ activities in sediment collected from paved road surfaces and attributed elevated activities in suspended sediments in streams as resulting from particles rapidly transported from urban areas. In these settings, ^{7}Be and ^{210}Pb$_{ex}$ activities may be higher in the buried-channel portions of the watershed with substantial impervious surfaces, in contrast to the open channel parts of the watershed, where streambank erosion processes become important. Understanding sediment sources and ^{7}Be and ^{210}Pb$_{ex}$ dynamics in urban settings could provide insight into particle-associated contaminant sources and transport processes affecting urban streams.

Here we examine sediment sources and transport processes and associated ^{7}Be, ^{210}Pb$_{ex}$, and ^{137}Cs in an urban watershed. We address three key questions: How do activities of ^{7}Be and ^{210}Pb$_{ex}$ vary in urban sediments by source type and in response to rain events? What do these activities tell us about the sources of sediment to urban streams? How do stream-channel dynamics affect activities of ^{7}Be and ^{210}Pb$_{ex}$ as sediment is transported from urban source areas with buried channels into open-channel downstream areas?

2. Materials and methods

2.1. Study area

To address the questions described above, we examined ^{7}Be, ^{210}Pb$_{ex}$, and ^{137}Cs activities for two locations in the Dead Run watershed, an urban watershed in Baltimore, Maryland (Fig. 1). One location was the upper part of the watershed where, except for two gullies in a small open space between roads, there are no open channels—all the natural stream channels were buried during urbanization. All surface runoff that enters the buried channel network through numerous storm drains exits to an open channel at the Alexander Avenue Culvert (herein called the "Alexander Culvert")(drainage area = 0.369 km^2) (Fig. 1). About one-half of this area is impervious (roads, rooftops, and parking lots) and the other half is non-impervious or open space (lawns, parks, and green space) (Table 1). The second sampling location was the area that drains from Alexander Culvert to the U.S. Geological Survey (USGS) stream gaging site (Dead Run near Catonsville, Maryland, USGS station ID 01589312), about 0.7 km downstream from Alexander Culvert ("Dead Run gage"; 1.63 km^2 drainage area). The drainage area at the gage, which includes the Alexander Culvert drainage, is 42% impervious and 58% open space (Table 1). The watershed drains the Piedmont physiographic province and is underlain by the Mount Washington Amphibolite subunit of the Baltimore Complex (Crowley, 1976) and by interbedded gravels, sands, silts, and clays of the Potomac Group in the upper reaches of the watershed.

Table 1
Classification of area draining to Alexander Culvert (0.37 km^2) and Dead Run gage (1.63 km^2).

	Contributing Area (km^2)	Percentage
Alexander Culvert	**0.369**	
Roads	0.048	13
Driveways	0.010	3
Residential Rooftops	0.028	7
Commercial Rooftops	0.028	8
Parking Lots	0.071	19
Total Impervious area	**0.185**	**50**
Other (parks, lawns, green space, etc.)	0.184	50
Dead Run Gage	**1.630**	
Roads	0.226	14
Driveways	0.044	3
Residential Rooftops	0.141	9
Commercial Rooftops	0.085	5
Parking Lots	0.191	12
Total Impervious area	**0.687**	**42**
Other (parks, lawns, green space, etc.)	0.947	58

Flow exits the Alexander Culvert and continues in an open channel to the Dead Run gage (Fig. 1). Two tributaries (T1 and T2, Fig. 1) enter Dead Run between Alexander Culvert and the Dead Run gage; these tributaries are buried channels in their upper reaches and exit at culverts to open channels. Several small storm drains also enter the channel from neighborhoods upstream of the gage. During the study, parts of Dead Run between the Alexander Culvert and tributary T1 were undergoing restoration to create a stabilized reach with an engineered riparian zone (Fig. 1; Fig. 2A). Although some disturbance of the channel may have occurred during the restoration, measures were taken during the restoration to reduce erosion, including pinning of erosion-control nets and fabric along the stream. Our results at the Dead Run gage are unlikely to have been compromised by these activities. Between the gage and the restoration area and along T1, channels are incised (Fig. 2B, C) with steep eroding streambanks and bed material that ranges from gravel and sands to fines.

Dead Run is one of many urban watersheds in Baltimore City and Baltimore County in a research network operated by the University of Maryland, Baltimore County (UMBC)–Center for Urban Environmental Research and Education (CUERE) (https://cuere.umbc.edu). Among the research objectives of the UMBC-CUERE program in Dead Run are to understand flow, sediment, and contaminant dynamics in urban settings using high-frequency sampling with in-stream sensors and high spatial-resolution numerical models (Duncan et al., 2017; Barnes et al., 2018; Kemper et al., 2019).

2.2. Rainfall, runoff, pavement, soil, streambank, and fluvial sediment

Rainfall, stormwater runoff, pavement sediment (road and parking lot particulates), soil, streambank material, and fluvial sediment (bed and SS) were collected during three periods:

1) summer (14 July–17 Aug., 2017); 2) fall (20 Oct.–10 Nov., 2017), and 3) winter/spring (27 Feb.–14 May, 2018) seasons.

2.2.1. Sample collection

Rainfall (n = 33 samples) was collected in two 9.5-L acid-washed plastic buckets placed ~ 1.5 m above the ground. Rainfall for the summer was collected at the USGS office in Catonsville, MD (6 km from the Dead Run gage), and for the other seasons was collected at a rain gage at the Dead Run gage. The rain sample was acidified with 10% hydrochloric acid (HCl) and transferred to 1-L bottles along with three 10% HCl rinses of the collection bucket prior to shipping to the USGS Sediment Radioisotope Laboratory in Menlo Park, CA, for ^{7}Be, ^{210}Pb$_{ex}$, and ^{137}Cs analysis. Runoff samples, as defined here, are stormwater runoff that occurs on impervious surfaces and contains sediment. Two types of runoff were sampled: stormwater runoff collected at the Alexander Culvert (n = 9 samples) and road runoff collected at road storm drains and parking lot storm drains (n = 8 samples). Both types of runoff were collected by submerging an 18.9-L bucket into the runoff (flow).

Pavement sediment samples (n = 85 samples) were collected at the beginning of each sampling season and after rainfall events at four road sites chosen to represent the range of road types present in the watershed (residential and commercial), and from one parking lot in the Alexander Culvert watershed (Fig. 1). Similar to Collins et al. (2011), pavement sediment was collected with a hand broom and dustpan from alongside the curb and upgradient of a storm grate and placed in a

Fig. 2. (A) Dead Run below Alexander Culvert in restored area (11 April, 2018); (B) Incision along tributary T2 showing upstream view (11 April, 2018); (C) Dead Run upstream of gage (9 November 2018); (D) Alexander Culvert samplers (29 July, 2017); (E) Dead Run samplers (29 July, 2017). [Photograph by A.C. Gellis, U.S. Geological Survey]

plastic bag. In order to obtain at least 3 g of fine sediment, the area swept varied between samples; and although each area was swept clean, it is likely that some sediment remained behind.

To estimate the mass of material present on pavement in the area draining to Alexander Culvert, sediment also was sampled 4 times with a high efficiency vacuum (Envirometrics Model HVS3 High-Volume Surface Sampler) (n = 39 samples). The vacuum, which is designed for sampling settled house dust at particle sizes 5 μm or larger, was fitted with a 12.5-cm-long, 1-cm-wide nozzle. Prior to outdoor sampling, controlled tests with the vacuum were done in the USGS Baltimore, MD, laboratory, where known masses of fine material (< 63 μm) were vacuumed. The HVS3 averaged 98.3% efficiency for the range of masses tested (Table S1), although wind and unevenness of the pavement surface may introduce variability when sampling outdoors. For two of the four vacuuming events, only the pavement sites used in the sweep samples (not including Street C) (Fig. 1) were vacuumed. For the other two vacuuming events, sites were selected randomly to cover the spatial extent of the Alexander Culvert drainage area. Each sample was collected by starting at the midpoint in the road and ending at the curb.

A sediment yield at each vacuum site was determined by dividing the sediment mass recovered by the area vacuumed, determined as the width of the nozzle (12.5 cm) multiplied by the road or parking lot length sampled (m). Yields are reported as a total (unsieved) sediment yield (g/m^2) and a fine (< 63 μm) sediment yield (g/m^2). We consider both of these yields as "potential sediment yields," as the entire mass of sediment may not be mobilized and transported from the pavement by any given rain event.

Soil samples were collected at nine sites (Fig. 1) in the Dead Run watershed. At each site, three to five subsamples were taken using a plastic spatula from the top 1 cm of surficial soil within 3 m of one another and composited. Four samples of streambank material were taken from eroding streambanks between the restored area and the Dead Run gage (Fig. 1). Prior to sample collection, the exposed surface of a streambank was scraped off and discarded. Each streambank sample is a composite of subsamples from 3 to 5 eroding streambanks collected from the bottom to the top of each streambank using a plastic hand shovel.

Fluvial sediment consisted of samples of SS and bed material. SS was collected at Alexander Culvert and the Dead Run gage (Figs. 1 and 2D,E) using passive samplers (Phillips et al., 2000). After a rainfall event, water (if present) and sediment were removed from the passive samplers and transferred to 18.9-L buckets.

Samples of bed material were collected at the Dead Run gage. Bed material was collected from the surface (< 1cm) of fine-grained channel deposits using a stainless-steel spatula. Sediment from at least five deposits was collected and composited into one sample. A bed sample was not collected at Alexander Culvert because the channel immediately below the culvert was a transport reach with a gravel bed devoid of fines for most of the collection period.

2.2.2. Sample analysis

All samples were transported to the USGS laboratory in Baltimore, MD, and refrigerated. Sediment for radionuclide analysis—pavement sediment, soil, bank material, decanted SS samples (following a minimum of 1 week of refrigeration and settling), and bed material—were wet-sieved with distilled deionized (DI) water using a 63-μm polyester sieve. The sieved slurry was collected in glass bowls and dried at 65 °C for 2 or more days. The dried fine sediment (< 63 μm) was removed with a plastic utensil and sent for analysis of fallout radionuclides, organic carbon content, and grain size.

Sediment samples were analyzed for ^{7}Be, ^{210}Pb, ^{226}Ra, and ^{137}Cs at the USGS Sediment Radioisotope Laboratory in Menlo Park, CA, using high-resolution germanium detector gamma spectrometers following methods described in Fuller et al. (1999) and Van Metre et al. (2004). Measured activities of ^{7}Be and ^{137}Cs were corrected for radioactive decay from the date of sample collection to the date of analysis. Excess $^{210}Pb_{ex}$ was calculated as the difference between the measured total ^{210}Pb and ^{226}Ra, which is determined from the short-lived intermediate gamma-emitting isotopes ^{214}Pb and ^{214}Bi. Method detection limits (MDLs) for ^{7}Be and $^{210}Pb_{ex}$ were 0.0067 Bq/g. The sample-specific detection limit for ^{7}Be was determined by correcting the MDL for decay and varied among samples (0.0117 to 0.0317 Bq/g) as a result of different times between sample collection and analysis. The MDL for ^{137}Cs was 0.0004 Bq/g.

The reported 1-sigma uncertainty in the measured radionuclide activity (σ1) was calculated from the random counting error of samples and background standard spectra at the 1 standard deviation level. Uncertainty in measured activity was typically within ±10% of the measured activity for total ^{210}Pb and ^{226}Ra, ±18% for ^{7}Be, and ±20% for ^{137}Cs. Uncertainty in unsupported ^{210}Pb was propagated from the uncertainties in total ^{210}Pb and ^{226}Ra activity and averaged ±20%.

Acidified rain samples were screened through 63-μm polypropylene mesh into a container along with three 10% HCl rinses of each shipping bottle and processed following the methods outlined in Conaway et al. (2013) and Nakano et al. (2008) to concentrate the radionuclides into a small volume. Briefly, 0.100 ml each of stable Pb and Be inductively coupled plasma mass spectrometry (ICP-MS) stock standard solutions (1000 μg/mL) was added to the acidified sample to determine recovery.

Five mL of 10% (wt/v) solution of ferric chloride was added to facilitate concentration of radionuclides by sorption of Pb and Be to iron hydroxide formed on raising pH. Samples were equilibrated on an orbital shaker for 48 h. Concentrated ammonium hydroxide was then added to increase pH to 10 and precipitate iron hydroxide to sorb both the stable and radioactive isotopes of Pb and Be. The iron hydroxide floc was recovered by centrifugation after settling and decanting off the overlying solution by siphon. The concentrated iron hydroxide was then dissolved in concentrated HCl and transferred to a tared bottle. Concentrations of the added stable Pb and Be yield tracers in rainfall samples were measured by ICP-MS. Recoveries averaged 95 ± 8% and 86 ± 6% for stable Pb and Be, respectively. A subsample was transferred and weighed into a polyethylene vial for radionuclide analysis by high resolution gamma spectrometry as described for sediment samples. Activities of ^{210}Pb and ^{7}Be in rainfall samples were corrected for the recovery yield of Pb and Be (ratio of measured to added mass of stable and Pb and Be) and the fraction of redissolved sample analyzed. This method assumes that the stable Pb and Be attain isotopic equilibrium with all fallout radionuclides in the sample such that the radioisotopes are recovered in the same proportion as the yield tracer. The resulting activity was then divided by volume of rain collected to yield activities in units of Bq/L. ^{137}Cs and ^{226}Ra were below detection limits in rain samples, indicating negligible contributions of ^{210}Pb and ^{7}Be from aeolian dust that may have entered the rainfall collector. Additionally, all ^{210}Pb activity in rainfall is considered unsupported ^{210}Pb ($^{210}Pb_{ex}$) because the supported activity defined by ^{226}Ra was not detectable.

Runoff samples were split in the laboratory to determine fallout radionuclide activities in whole water and in isolated particulates. One split was churned and an aliquot was taken to determine the suspended-sediment concentration (SSC). The volume of the aliquot was recorded and the aliquot was pumped through a 0.45-μm glass fiber filter. The filter was dried at 105 °C and weighed. The remaining slurry from this split was processed for analysis in the same manner as SS from the passive samplers to record activity in the particulates in Bq/g. A second split was prepared and analyzed in the same way as rainwater to measure "total" whole-water ^{7}Be and $^{210}Pb_{ex}$ activities. It was assumed that ^{7}Be and ^{210}Pb are effectively solubilized from the SS at the low pH of the acidified sample. It also was assumed that isotopic equilibrium is attained between yield tracers (stable Pb and Be) and ^{7}Be and ^{210}Pb both in solution and on sediments. ^{210}Pb activity in "total" whole-water runoff samples is considered unsupported ^{210}Pb ($^{210}Pb_{ex}$) because the supported activity defined by ^{226}Ra was not detectable. Reported activities in the whole-water samples in units of Bq/L were normalized to SSC to obtain units of Bq/g. Additional analytical methods for sediment are shown in SI Text I.

2.2.3. Collection and computation of rainfall, turbidity, suspended sediment, and flow

UMBC operates a rainfall and water-quality network in the Baltimore Metropolitan region that includes Dead Run. Water-quality sensors and a rain-gage station are co-located with USGS stream gage 01589312.

The collection and computation methods for rainfall, turbidity, suspended sediment, and flow are described in SI Text II.

2.3. Potential activity of ^{7}Be and $^{210}Pb_{ex}$

We used measured activities of $^{210}Pb_{ex}$ and ^{7}Be in rainfall, potential sediment yields from pavement, and $^{210}Pb_{ex}$ and ^{7}Be activities in pavement sediment measured prior to the rainfall event to estimate the enrichment of pavement sediment that might occur (potential activity) in response to a rainfall event. The potential activity of ^{7}Be and $^{210}Pb_{ex}$ in the sweep samples after being tagged by rainfall was determined as:

$$RDSED_{pot\,(t)} = \frac{(RAIN_{tot} * RAIN_{act})}{SED_{yld}} + \mathrm{RDSEDpre} \tag{1}$$

where $RDSED_{pot(t)}$ is the potential activity of ^{7}Be or $^{210}Pb_{ex}$ in pavement sediment for sample period *t* as a result of precipitation (Bq/g); $RAIN_{tot}$ is the total rainfall over 1 m^2 of the ground surface (L/m^2); $RAIN_{act}$ is the measured activity of ^{7}Be or $^{210}Pb_{ex}$ in rainfall (Bq/L); SED_{yld} is the median fine sediment yield from vacuuming (g/m^2) = 1.57 g/m^2 (Clifton et al., 2019); and $RDSED_{pre}$ is the pavement sediment activity for ^{7}Be or $^{210}Pb_{ex}$ (Bq/g) prior to the rainfall event and corrected for ^{7}Be decay since the time of the last pavement sediment sweep.

Because of the strong affinity of ^{7}Be and $^{210}Pb_{ex}$ to fine particulate matter (Benmansour et al., 2014; Taylor et al., 2012), we assume that all whole-water runoff samples have an activity per liter (Bq/L) equal to rainfall, and that some of the ^{7}Be and $^{210}Pb_{ex}$ are likely sorbed to particles and surfaces that are not transported with runoff to the culvert. The calculation therefore provides an upper limit for radionuclide tagging.

2.4. Sediment sourcing

Pavement sediment can be from a mixture of sources, including upland soil from lawns and open space, building and construction material, leaf litter, atmospheric deposition of particles, worn tires, and pavement erosion (Taylor and Owens, 2009; Sansalone and Cristina, 2004). A two-endmember mixing model using ^{137}Cs as a tracer was used to calculate soil and non-soil sources to pavement sediment. One endmember is soil, with an activity equal to the median of the ^{137}Cs activity in soil samples (0.0071 Bq/g) (Clifton et al., 2019). The non-soil endmember is assigned zero activity under the assumption that the non-soil material is from sources such as construction materials and tire and asphalt wear that are not expected to have detectable ^{137}Cs activity. The percentage of pavement residue originating from soil was determined as:

$$Soil\% = Cs_{sample}/Cs_{med} * 100 \tag{2}$$

where *Soil%* is the percentage of the sample that is derived from soil, Cs_{sample} is the ^{137}Cs activity (Bq/g) of the sample, and Cs_{med} is the median of the ^{137}Cs activities in the soil samples (0.0071 Bq/g).

To determine sources of SS samples collected from Alexander Culvert and SS and bed sediment at Dead Run, an unmixing model commonly used in sediment source studies was applied:

$$\mathrm{Res} = \sum_{i=1}^{n} \left[\frac{Cssi - (\sum_{s=1}^{m} CsiPs)}{Cssi} \right]^2 \tag{3}$$

where Res is the residual sum of squares, *Cssi* is the concentration of tracer property *i* in the target sediment, *Csi* is the mean concentration of the tracer property in the source group *s*, and *Ps* is the relative contribution from source group *s* (after Walling, 2005; after Schuller et al., 2013).

The unmixing model equation assumes that $0 \le \mathrm{Ps} \le 1$ and

$$\sum_{s=1}^{m} Ps = 1 \tag{4}$$

The P_s that yields the lowest residual sum of squares corresponds to the final source contributions (pavement, soil, banks) for a given target sample.

3. Results and discussion

3.1. Rainfall and flow during the study

Rainfall, pavement, and fluvial samples were collected for 17 sampling periods over a range of flows distributed over the three sampling seasons (Fig. 3; Table 2; SI Table S2). A sample period begins after the last sample is collected from the previous sampling period (the end of a rainfall event) and ends when the last sample of the current sampling period is collected (also a rainfall event). Samples collected during each sampling period can include pavement sweeps (dry weather) and

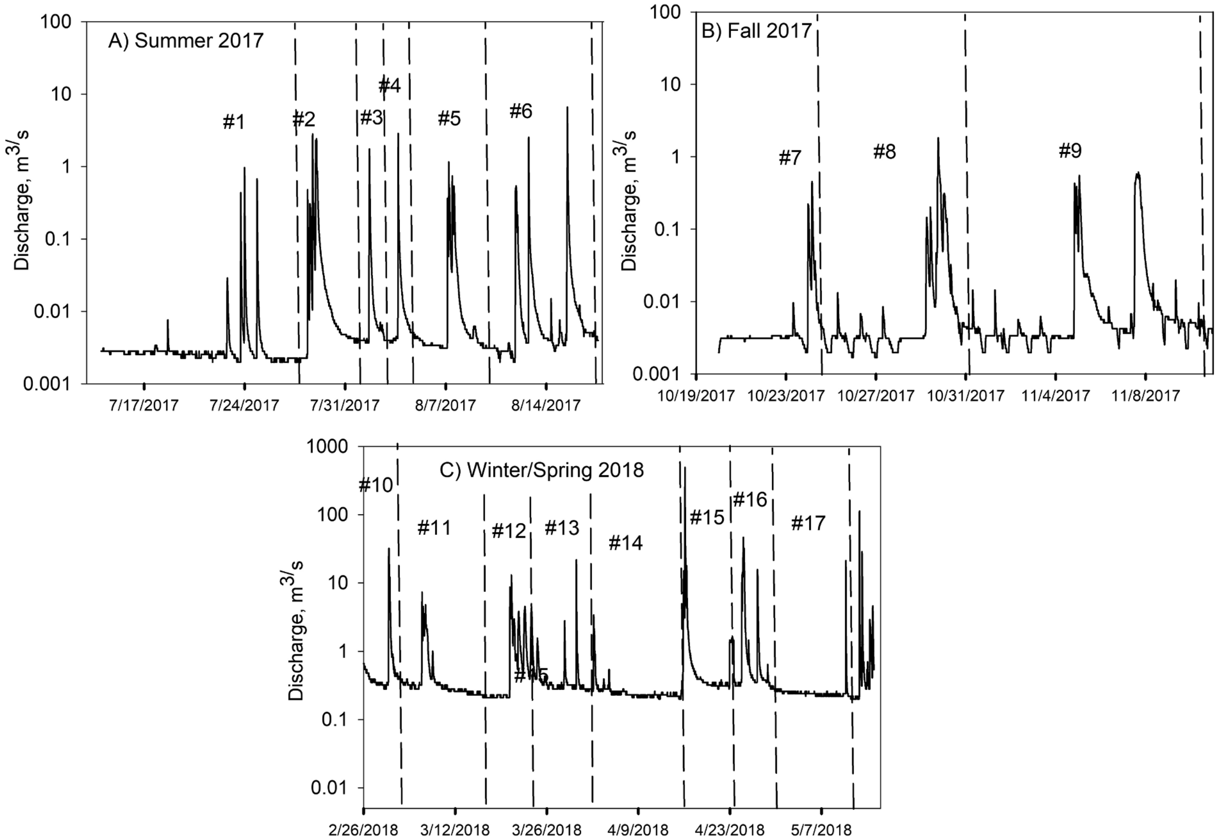

Fig. 3. Summary of flow events at Dead Run gage (USGS station ID 01589312) for the 17 sampling periods in this study in (A) Summer 2017, (B) Fall 2017, and (C) Winter/Spring 2018 (data available at U. S. Geological Survey, 2019).

rainfall, runoff, and suspended and bed sediment from one or more rainfall events. A sampling period had as many as one to five peak flows, depending on how closely spaced the rainfall events were (Table 2). The decision to collect samples was based on rainfall and discharge. The lower sediment tube at Dead Run gage filled at a discharge of about 0.19 m^3/s. When it rained, we examined the on-line real time discharge at Dead Run; if it exceeded 0.19 m^3/s the decision was made to retrieve SS samples, if conditions permitted (low flow). Street sweeps were collected only when conditions were dry. Additional rainfall event(s) did occur before it was possible to get street sweeps during some sampling periods, and thus a sampling period may have had multiple rainfall and SS samples but only one set of sweep samples.

Table 2
Hydrologic summary of sampled events at Alexander Culvert and Dead Run Gage. * Indicates a stormwater runoff sample(s) was taken at Alexander Culvert and ǂ indicates a road runoff sample(s) was taken during a given sampling period.

Sampling period start date	Sampling period start time	Sampling period end date	Sampling period end time	Total Rain (mm)	Number of flow events in this period at Dead Run gage	Highest peak flow during sample period, (m^3/s)	Total Suspended Sediment Load, (Mg)
Summer 2017							
7/14/2017	13:40	7/27/2017	14:35	21.3	4	0.96	1.3
7/27/2017	14:35	8/1/2017	13:30	96.2	4	2.81	3.4
8/1/2017	13:30	8/3/2017	12:30	5.4	1	1.75	0.59
8/3/2017	12:30	8/4/2017	10:30	7.5	1	2.86	2.1
8/4/2017*	10:30	8/10/2017	10:20	25.3	3	1.16	1.1
8/10/2017	10:20	8/17/2017	09:30	51.8	3	2.54	7.0
Fall 2017							
10/20/2017	13:00	10/24/2017	13:45	6.3	2	0.46	1.0
10/24/2017*ǂ	13:45	10/31/2017	11:30	37.3	4	1.84	5.1
10/31/2017*ǂ	11:30	11/10/2017	11:46	39.4	2	0.61	4.2
Spring 2018							
2/27/2018	12:00	3/6/2018	12:50	16.6	2	0.90	1.2
3/6/2018	12:50	3/19/2018	12:00	13.1	1	0.21	0.19
3/19/2018	12:00	3/26/2018	11:40	snow	5	0.62	0.79
3/26/2018*	11:40	4/4/2018	13:05	12.7	3	1.32	0.52
4/4/2018	13:05	4/18/2018	13:55	53.5	1	14.0	19.9
4/18/2018	13:55	4/26/2018	13:45	32.1	3	1.31	2.7
4/26/2018	13:45	5/2/2018	15:40	8.41	1	0.44	0.22
5/2/2018	15:40	5/14/2018	15:50	28.8	3	3.20	2.9

Often because of high-flow conditions it was not possible to access the suspended sampler immediately at the end of the event, and in some of these cases a second flow event occurred (Table 2) during the same sampling period and the sampler composited suspended sediment over more than one closely spaced rainfall event. Rain samples were collected during 16 of the 17 sampling periods and analyzed for radionuclides. Seventeen runoff samples (9 stormwater samples at Alexander Culvert and 8 stormwater samples from roads) were collected during 4 of the 17 sampling periods (Table 2). Of the 9 runoff samples collected at Alexander Culvert, 7 were used for whole-water analysis (Bq/L), and 6 were used for dry sediment analysis (Bq/g). Of the 8 runoff samples collected on roads, 7 were used for whole water analysis (Bq/L) and 5 were used for dry sediment analysis (Bq/g) (Clifton et al., 2019).

To determine if any of the seasons sampled were drier or wetter than average, rainfall for each sampling season was compared to the historic rainfall for the same season measured at the National Weather Service gage at the Baltimore/Washington International Airport (USW00093721), 16.2 km from the Dead Run gage (Table S3). The three seasons had rainfall that was 179% (summer), 137% (fall), and 70% (winter/spring) of normal rainfall for that season (Table S3). The wetter summer and fall seasons could affect the results by supplying more sediment than might occur during average rainfall conditions or could cause higher flows that exhaust sediment in channel storage. Conversely, samples collected during the drier winter/spring season might reflect lower sediment flux than might occur during average rainfall conditions.

3.2. Radionuclide activities in source and collected sediment samples

The three types of source material—pavement sediment, upland soil, and streambanks—have characteristic activities of ^{7}Be, ^{210}Pb$_{ex}$, and ^{137}Cs that reflect differences in initial (pre-rain) activities and the timing and intensity of radionuclide tagging and dilution (Clifton et al., 2019). Activities of ^{137}Cs were higher in soils than in streambank material, and similar to, or higher than, those in pavement sediment (Fig. 4). Fallout of ^{137}Cs for North America largely ceased by the late 1960s (Ritchie and McHenry, 1990), and soil now is a reservoir of legacy ^{137}Cs from past fallout. Variable ^{137}Cs activities in pavement sediment likely reflect varying contributions of upland soil to the sediment on the impervious surface. Significant differences in activities of ^{137}Cs (as well as ^{210}Pb$_{ex}$ and ^{7}Be) among some of the pavement sediment sites (Mann-Whitney Rank Sum test ($p < 0.05$)) (Table S4) likely reflect different source contributions to sediment at a site. The detection of ^{137}Cs activity in some streambanks indicates that these samples do not represent older alluvial deposits, which should be devoid of ^{137}Cs, but may indicate deposition from eroded topsoil that occurred when

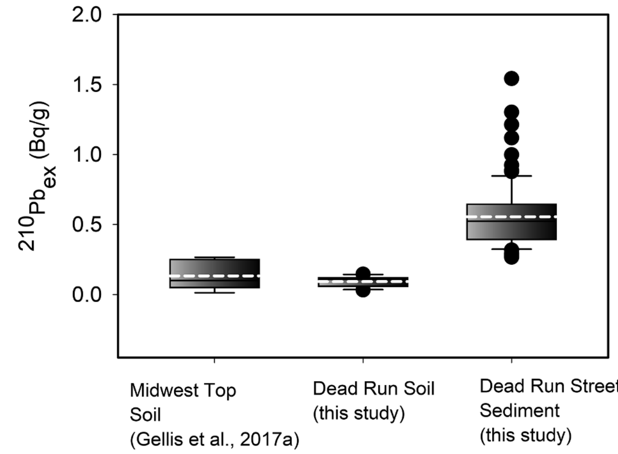

Fig. 5. Comparison of ^{210}Pb$_{ex}$ in Midwest topsoil, Dead Run soil, and street sweeps.

parts of the Dead Run watershed were developed between the 1950s and 1970s. The median year for homes built in the Dead Run watershed was 1962 (Barnes et al., 2018), which is one year earlier than the peak fallout of ^{137}Cs. Thus topsoil mobilized during the build out of the area would have contained relatively high ^{137}Cs, which could have been deposited on the floodplain.

In contrast to ^{137}Cs, ^{210}Pb$_{ex}$ and ^{7}Be are continually deposited on the land surface by atmospheric fallout, resulting in distinct signatures of these two radionuclides in the three sediment sources. Activities of ^{210}Pb$_{ex}$ and ^{7}Be were substantially higher in samples of pavement sediment than in samples of upland soil and streambank material (Fig. 4A,B). The difference between activities in pavement sediment and streambank material is consistent with the limited exposure of streambanks to modern atmospheric fallout (Gellis et al., 2017b; Hancock et al., 2014; Matisoff et al., 2005). The soil activities of ^{210}Pb$_{ex}$ in Dead Run watershed are similar to those reported for agricultural topsoil in the Midwest (Gellis et al., 2017b) (Fig. 5). The difference between activities in pavement sediment and upland soil (Fig. 5) reflects the difference in the mass of sediment exposed to rain. On pavement, a thin veneer of sediment is exposed to a relatively large volume of rain whereas for soil, the top several centimeters are exposed. As a result, on a per gram basis, pavement sediment receives greater amounts of radionuclides (resulting in higher activities) during a rain event than does soil.

Activities of ^{210}Pb$_{ex}$ and ^{7}Be in pavement sediment are correlated ($r^2 = 0.51$; Fig. S2A) because they both are delivered to the Earth's

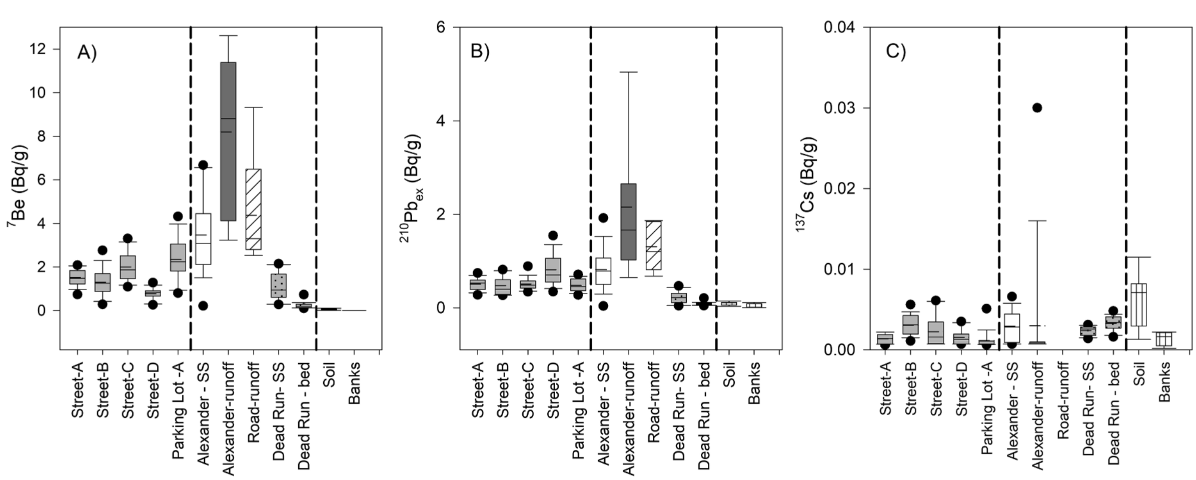

Fig. 4. Summary of radionuclide activity in sediment (Bq/g) for all samples (A) ^{7}Be, (B)^{210}Pb$_{ex}$, and (C) ^{137}Cs Table S2; Clifton et al., 2019).

surface by rainfall and both associate with particles (McNeary and Baskaran, 2003; Matisoff et al., 2005). In contrast, $^{210}Pb_{ex}$ in pavement sediment is not correlated with activities of ^{137}Cs (Fig. S2B (r^2 = 0.12)) and suggests a fundamental difference between pavement sediment and soils (Fig. 5). However, $^{210}Pb_{ex}$ and ^{137}Cs are strongly correlated in soils (Wallbrink and Murray, 1996; Huh and Su, 2004; Porto et al., 2010; Teramage et al., 2013). Porto et al. (2010) suggested that the close relation of $^{210}Pb_{ex}$ and ^{137}Cs activities in soils reflects a similar and consistent response to erosion and sediment redistribution processes. Pavement sediment, which is transported away and replenished over short time scales, does not undergo such processes. We interpret the lack of correlation between $^{210}Pb_{ex}$ and ^{137}Cs activities in pavement sediment as resulting from tagging of pavement sediment by recent fallout of $^{210}Pb_{ex}$ (and ^{7}Be) but not of ^{137}Cs.

Activities of ^{7}Be, $^{210}Pb_{ex}$, and ^{137}Cs in runoff, SS, and bed samples are expected to be bracketed by those in the sediment sources (pavement sediment, soils, and, for Dead Run, streambanks). Activities of ^{137}Cs in fluvial sediments collected at Alexander Culvert and Dead Run are within the range of source sediment (pavement sediment, upland soil, and streambank material) (Fig. 4C). Activities of ^{7}Be and $^{210}Pb_{ex}$ in SS at Alexander Culvert, however, are similar to or greater than those in the assumed source materials (Fig. 4A,B). The explanation for this is presented in section 3.3.

3.3. Radionuclide activity by event

Activities of $^{210}Pb_{ex}$ and ^{7}Be are highest in particles in runoff (Alexander and road runoff), followed by SS at Alexander Culvert and pavement sediment (Figs. S3A–C). The amount of enrichment of ^{7}Be and $^{210}Pb_{ex}$ in runoff and Alexander Culvert SS relative to the pavement

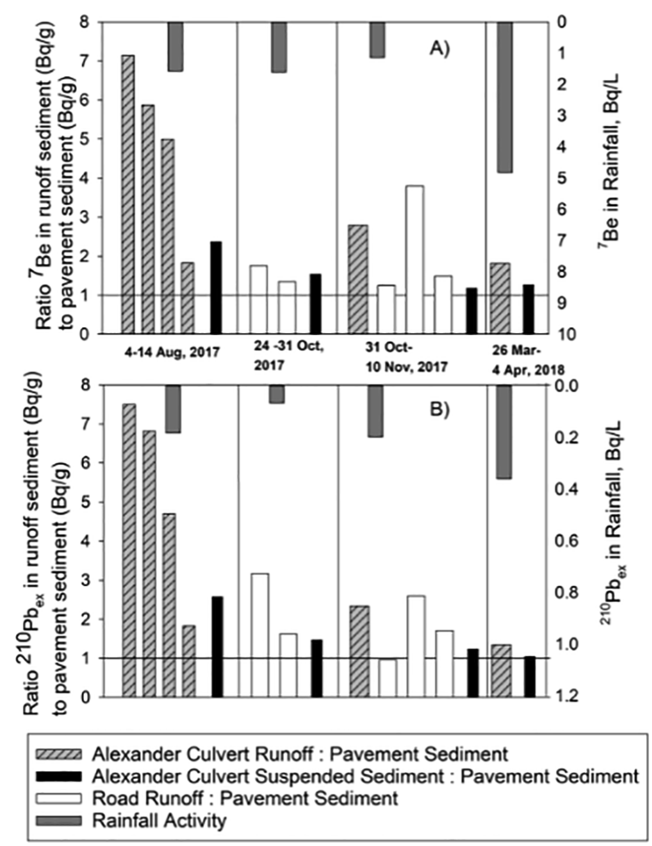

Fig. 6. Activity ratios of (A) ^{7}Be (B) and $^{210}Pb_{ex}$ in sediment from runoff samples (Alexander Avenue Culvert runoff and road runoff) to Alexander Culvert suspended sediment and pavement sediment. Solid gray bars represent rainfall activity.

sediment samples can be quite large, as indicated by the ratios of these activities for the four runoff periods sampled to pavement sediment-sample activities (Fig. 6). We hypothesize that the difference in activities provides critical insight into the dynamics of $^{210}Pb_{ex}$ and ^{7}Be particle tagging at the scale of an urban watershed and explains why the fluvial sample $^{210}Pb_{ex}$ and ^{7}Be activities are not bracketed by the source activities.

Rainfall-runoff entrains a relatively small mass of particles in suspension, which comes in contact with a relatively large volume of precipitation, leading to enrichment in particle-associated radionuclides carried by the rainfall/runoff. The mass of particles that remains on the pavement also is exposed to rainfall, but the ratio of rainfall volume to pavement sediment mass is smaller, resulting in less enrichment on a per particle-mass basis. By extension, soil, with its much greater mass of particles and downward diffusion of rainwater through infiltration, is even less enriched by a given rainfall event than are pavement particles (Fig. 5). One of the four rainfall events sampled (2 August, 2017) included runoff samples collected in Alexander Culvert shortly after the onset of rainfall (Figs. S3Aix-xi; S4); for that event, ^{7}Be activity of sediment in runoff samples decreased through the event (12.6, 10.4, 8.81, 3.24 Bq/g) (Fig. S3-Ax). A similar pattern was observed for $^{210}Pb_{ex}$ (2.65, 2.41, 1.66, 0.65 Bq/g) (Fig. S3Axi). Delivery of ^{7}Be has been observed to decrease rapidly during a rain event, a process attributed to scavenging and washout of radionuclides from the atmosphere (Caillet et al., 2001; Ioannidou and Papastefanou, 2006; Gourdin et al., 2014). Thus, the earlier part of the runoff period would have higher radionuclide tagging of sediment than later in the event. Decreasing activities of ^{7}Be and $^{210}Pb_{ex}$ relative to the onset of rainfall could be related to the washout of those radionuclides during an event (Fig. S5). However, the composite rainfall samples collected by this study do not allow for an evaluation of rainfall activities over the course of the event. Furthermore, fallout radionuclide activity during a storm can be influenced by other factors, such as cloud height, storm types and duration, and seasonality (Todd et al. 1989; Kaste et al., 2002; Karwan et al., 2016).

Another potential explanation for the higher activities in the Alexander Culvert runoff and SS samples versus other sources is grain size and organic content differences among the sample types. The activity of radionuclides has been shown to increase with decreasing sediment size (Taylor et al., 2014; He and Walling, 1996) and increasing organic content (Navas et al., 2011; Motha et al., 2002). Examination of grain size (D_{50}) and organic content (total organic carbon %; TOC) among sample types does not indicate that the Alexander Culvert SS has finer grain sizes or higher TOC content (Fig. S6), and thus neither grain size nor organic content explain the higher activities in the Alexander Culvert runoff and SS samples relative to sediment sources. Froger et al. (2018) also did not observe any relation between sediment grain size and ^{7}Be and $^{210}Pb_{ex}$ activities for an urban area in France.

3.4. Sediment sources

A two-endmember model using ^{137}Cs (Eq. (2)) determined the sources of pavement sediment and indicates a soil contribution to the pavement sediment samples (n = 85) of 26 ± 23%. The high variability within the source contributions reflect the heterogeneity of pavement sediment and is consistent with other studies that have reported a wide range of soil and/or inorganic sediment on impervious surfaces (Loganathan et al., 2013; Sartor et al., 1974; Fergusson and Ryan, 1984).

Sediment sources to suspended sediment collected at Alexander Culvert and suspended and bed sediment collected at Dead Run were apportioned using an unmixing model (Eqs. (3) and (4)) with three tracers (^{7}Be, $^{210}Pb_{ex}$, ^{137}Cs) and the results averaged (Table 3; Table S5). Several metrics (mean, median, 90th percentile) were tested for each endmember. The pavement sediment endmember was assigned the median pavement sediment activities for ^{137}Cs (0.0015 Bq/g), and

Table 3
Summary of source contributions to fluvial sediment samples using an unmixing model (Eqs. (3) and (4)) (SI Table 5). Values are mean percentage and standard deviation in parenthesis. * The fallout radionuclide (FRN) activity of fluvial sediment draining to the Alexander Culvert is similar to FRN activity at Dead Run.

Fluvial sediment type	Pavement	Soil	Banks and other FRN free material
Alexander suspended sediment	45(25)	22(19)	32(35)*
Dead Run suspended sediment	15(9)	28(7)	57(15)
Dead Run bed sediment	4(2)	39(11)	57(12)

the median activities from runoff for $^{210}Pb_{ex}$ (1.638 Bq/g) and ^{7}Be (4.121 Bq/g), assuming that these runoff particles more reasonably represent activities of pavement sediment that is transported to the stream. Because pavement sediment is not currently subject to fallout of ^{137}Cs, we believed it adequately reflected ^{137}Cs activities in runoff. Median radionuclide activities were used for the soil endmembers (^{137}Cs = 0.0071 Bq/g; $^{210}Pb_{ex}$ = 0.1070 Bq/g; ^{7}Be = 0.0611 Bq/g) and values were set to one-half the detection levels for the streambank (and other fallout-radionuclide-free material) endmember ($^{210}Pb_{ex}$ = 0.0033 Bq/g; ^{7}Be = 0.0050 Bq/g; ^{137}Cs = 0.0002 Bq/g). Low fallout radionuclide activities in some target samples indicate that a low-activity, or fallout-radionuclide-free, endmember is supplying sediment in spite of the detection of ^{137}Cs, and to lesser extent $^{210}Pb_{ex}$, in bank samples collected for this study.

Large variation in activities of the endmember and target samples resulted in large variability (>20%) in source proportions for the Alexander SS samples (Table 3). Target samples should be bracketed by the source sample activities (within 10% of the minimum and > 10% of maximum activity) (Gellis and Gorman Sanisaca, 2018). In 4 of 57 target samples, the sample activities of $^{210}Pb_{ex}$ (n = 1) and ^{7}Be (n = 4) were outside the range of endmember activities in a direction that implies a mix of soil and pavement sediment, the two higher activity sources (Fig. 7). All four target samples were Alexander Culvert SS, which had relatively high activities of ^{7}Be and $^{210}Pb_{ex}$. One possible explanation for the activities in these samples is that the soil in suspension in runoff is being tagged by rainfall radionuclides in the runoff, similar to the tagging of the pavement sediment.

The model results indicate that pavement sediment is the dominant sediment source in the buried channel part of the watershed at Alexander Culvert, and that downstream at Dead Run, where the channel is open, streambank sediment dominates. The unmixing model

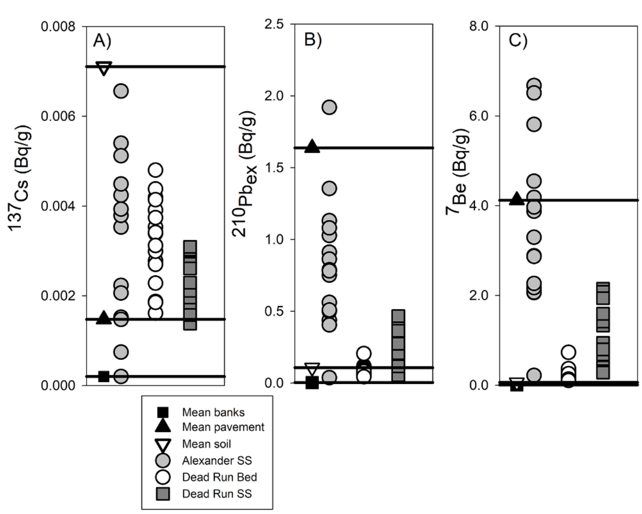

Fig. 7. Mean ^{137}Cs, $^{210}Pb_{ex}$, and ^{7}Be source endmembers (banks, soil, pavement) plotted with fluvial (target) samples at Alexander Avenue Culvert and Dead Run gage. [SS = suspended sediment]

results in a mean pavement contribution at Alexander Culvert of 45 ± 25% in SS samples, with a contribution from older channel material of 32 ± 35%, and the remainder coming from soils (22 ± 19%) (Table 3). These relatively large contributions of pavement sediment are consistent with the ranges of $^{210}Pb_{ex}$ and ^{7}Be in pavement sediment, runoff, and Alexander Culvert samples (Fig. 7) and with the nature of the contributing watershed.

The Dead Run gage site sampled the open channel portion, thus all three potential sources are expected. Based on the unmixing model, the mean fraction of pavement sediment is 15 ± 9% in Dead Run SS and 4 ± 2% in bed sediment. The decrease in the pavement-sediment contribution from Alexander Culvert to Dead Run indicates relatively rapid dilution of the pavement-sediment fraction downstream from where buried channels emerge into open channels. The dilution is from streambanks, which contributed 57 ± 15% of the Dead Run SS and 57 ± 12% of the Dead Run bed sediment.

Counterintuitively, the model results indicate an average of 32 ± 35% streambank contribution to Alexander Culvert SS, with very high variability between sampled events. Because the culvert emerges from buried channels with no exposed streambanks, there should be only two major sources possible: soil and pavement sediment. We interpret the modeled component of streambank material at the culvert as older channel material and subsoil eroded from within the culvert system. In many urban areas, stream channels have been buried in pipes, culverts, and combined sewer systems (Broadhead and Lerner, 2013; Broadhead et al., 2015; Elmore and Kaushal, 2008). The breakup, cracking, and wear of these underground pipes and culverts is common and leads to openings that allow the surrounding soil to enter the pipe (infiltration) (Tang et al., 2018; Sato and Kuwano, 2015; Ellis, 2001). The continued erosion of the soil forms a cavity and in some cases leads to sinkholes (Ali and Choi, 2019; Sato and Kuwano, 2015; Tang et al., 2018). We hypothesize that the bank source contributions observed in our model output at Alexander Culvert reflect buried channel sediment entering the culvert through openings. Further studies that examine sediment transport and the condition of underground pipes in areas of buried channels may help to resolve this question, and radionuclide analyses, such as done here, could indicate culvert systems subject to underground failures.

Sediment budgets from the literature that quantify sediment sources in urban watersheds indicate that the contribution from impervious areas ranges from 4 to 46% (Table S6), covering the range in pavement sediment contributions to fluvial sediments from the Alexander Culvert (45%) and Dead Run gage (4 to 15%) (Table 3). Contributions from soil (22 to 39%) and streambank (and other fallout-radionuclide-free material, i.e., older channel deposits) (32 to 57%) sources at Dead Run are also within the range reported for other urban areas (Table S6).

Because pavement sediment is a vector for metals, PAHs, and other urban contaminants (Van Metre and Mahler, 2003; Mahler et al., 2005; Callender and Rice, 2000), its proportion in fluvial sediment is an indicator of the contribution of pavement sediment to sediment contamination. The high percentage of pavement sediment at Alexander Culvert indicates the potential for contaminant "hot spots" where culverts and buried channels discharge to urban streams. Although the fraction of pavement sediment decreases rapidly with distance downstream, it nonetheless accounts for about one-third or more of

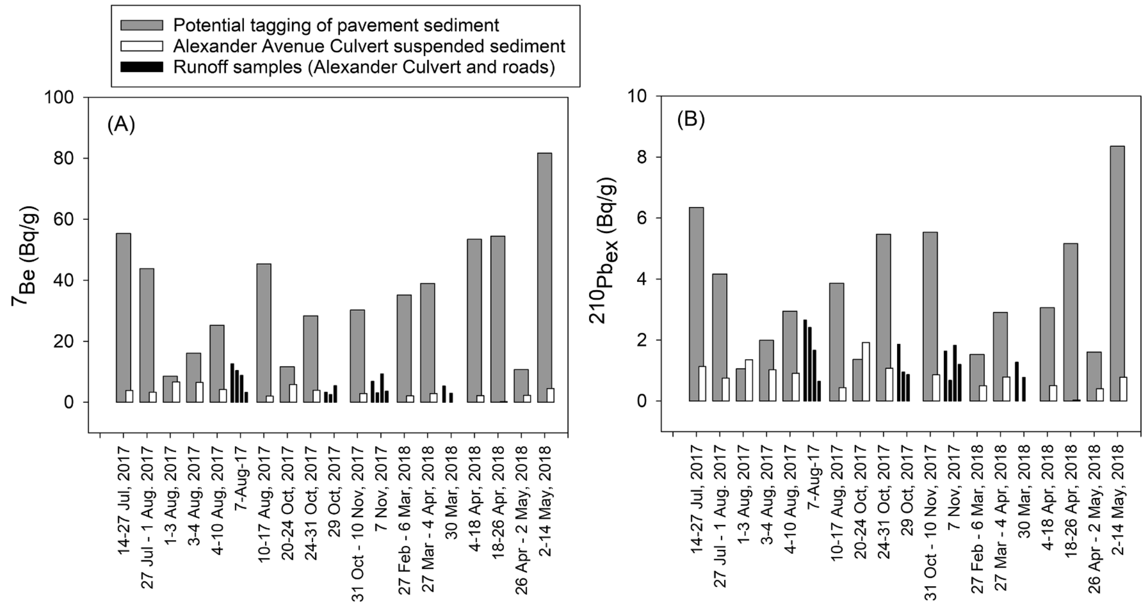

Fig. 8. Potential tagging of pavement sediment for (A) ^{7}Be and (B) ^{210}Pb$_{ex}$ compared for Alexander Avenue Culvert SS samples and runoff samples.

suspended sediment in some samples at the Dead Run gage.

3.5. Potential radionuclide tagging of pavement sediment

Based on Eq. (1), the potential activity of ^{7}Be and ^{210}Pb$_{ex}$ added to pavement sediment by tagging from rain events is more than sufficient to account for the sediment activity measured in the runoff and the Alexander Culvert SS samples (Fig. 8). Activities in runoff samples and rain samples are also compared using whole-water units of measurement (Bq/L; activity/volume) (Table S7), which avoids the large uncertainty in the pavement-sediment yields. Activities of ^{210}Pb$_{ex}$ and ^{7}Be in rain are substantially greater than those in whole-water samples of runoff for the same event (Table S7). Although the rainfall samples reflect rainfall collected over a longer time than represented by the runoff and the runoff samples represent a single point in time, the data are consistent with the hypothesis that a substantial part of the rainfall load of ^{7}Be and ^{210}Pb$_{ex}$ does not exit the system but is retained within watershed soils, pavement surface, or other solid surfaces.

3.6. Urban pavement sediment yields

The total potential sediment yield determined from vacuuming (sand and fines) averaged 55.6 ± 97.2 g/m^2 and the fine-sediment potential yield averaged 5.9 ± 11.7 g/m^2 ($n = 39$). The high variability and skewness (figs. S7A,B) are consistent with those reported for other studies (Sartor et al., 1974). The median total sediment yield 15.4 g/m^2 and fine sediment yield of 1.57 g/m^2 were used in further analysis. Parking lot samples had significantly lower total and fine sediment yields than road samples (Mann-Whitney Rank Sum test, $p = 0.003$) (Figs. S7A, B). Pavement sediment yields determined for this study are comparable to those reported by Waschbush (2003) and by Selbig and Bannerman (2007) but are greater than those reported by Mahler et al. (2005) (Figs. S7-C). Most of the pavement sediment mass is sand sized (mean percentage of material < 63 µm of 16.1 ± 16.9%), a grain size commonly found in urban environments (Sartor et al., 1974; Waschbush, 2003; Selbig and Bannerman, 2007; Taylor and Owens, 2009).

Could pavement sediment constitute a substantial part of stream sediment in an urban environment? Wolman (1967) presented a conceptual model where sediment yields in an urban environment were projected to decrease after development, related to the loss of upland sediment source areas. Contrary to this expected decline in sediment yield as urban areas expand, Gellis et al. (2017a), Cashman et al. (2018) found that sediment yields for Difficult Run, an urban/suburban watershed in Virginia outside of Washington, D.C., remained high even after 30 or more years had passed since peak rates of urbanization. Both studies attributed the high sediment yields to streambank erosion.

To determine the potential sediment load and yield available on impervious services, the median total and fine yields from the vacuum samples were extrapolated to the total impervious area of roads and parking lots in the Dead Run gage (0.42 km^2) (Table 1). The results indicate that about 6.4 and 0.65 Mg of total and fine sediment, respectively, are present on impervious surfaces in the Dead Run watershed at any given time. The average annual SS load at the Dead Run gage (2013–2016) is 127 Mg (Kemper et al., 2019). Three events sampled for percent fines in Dead Run at Catonsville and surrounding gages (Table S8) indicated that on average 91% of the suspended sediment is < 63 µm.

If the same ratio of fines and sand in suspended sediment is applied to the impervious surface sediment, then 0.71 Mg of sediment is available for transport, which is a very small percentage (0.6%) of the total annual suspended-sediment load measured at the Dead Run gage. However, this relatively small mass represents the potential sediment available at any one time on roads and parking lots and it is likely that only a part of this impervious sediment is mobilized in a given flow event. To estimate the total mass of impervious sediment mobilized in a given year from all events, we first defined an event as when peak flow exceeds the 90th percentile of all 5-minute discharges for the 2017 and 2018 study period (0.032 m^3/s). Using this definition, 68 flow events occurred. Sediment delivery in urban watersheds can be high (Russell et al., 2019), and in watersheds with impervious areas similar to Dead Run (50%) the sediment delivery ratio is ~50% (Heathcoate, 2009). If we assume that 50% of the impervious sediment is mobilized and delivered to the stream, the estimated total contribution of the 68 events is 24 Mg, or 19% of the annual sediment load. Our results suggest that the sediment available for transport from roads and parking lots has the potential to be an important contributor to the total sediment load in an urban stream as well as an important contributor of contaminants. We recognize that values assigned to define an event and to estimate the percentage of sediment mobilized on impervious surfaces were arbitrary. The actual mass available for transport, mobilized from impervious areas, and delivered to the stream would require systematic

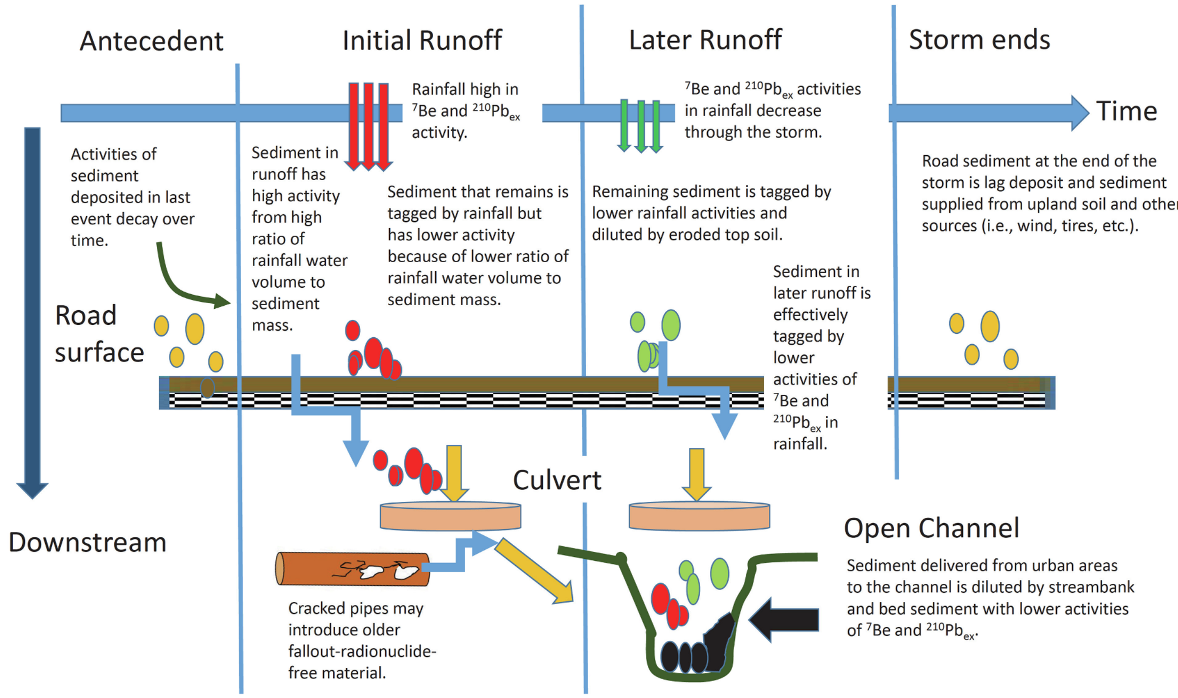

Fig. 9. Conceptual diagram illustrating how fallout radionuclide activities change along the transport cycle of sediment through the urban environment. The different colors of the sediment indicate changes in radionuclide labelling over time.

event-based monitoring over time, which was beyond the scope of this study. However, this estimate of pavement sediment determined using the sediment yield provided by the vacuum cleaner results (19%) is similar to the pavement sediment contribution results from the unmixing model (15%) for Dead Run SS (Table 3), indicating our assumption of 50% mobility in a given event is reasonable.

3.7. Conceptual model

We propose a conceptual model based on the activities of ^{7}Be and ^{210}Pb$_{ex}$ in rain, runoff samples, pavement sediment, topsoil, and fluvial samples, that describes how activities of ^{7}Be, ^{210}Pb$_{ex}$, ^{137}Cs in sediment change as sediment is transported in an urban setting (Fig. 9). Antecedent conditions control the initial ^{7}Be and ^{210}Pb$_{ex}$ activity of pavement sediment before a rainfall-runoff event occurs, as reflected by the activities of the pavement-sediment samples collected prior to rain events. This initial activity is a function of ^{7}Be and ^{210}Pb$_{ex}$ activity tagging from previous events, dilution from deposition of other material with lower activities of those radionuclides during and between events, and decay of ^{7}Be since the last event (decay is negligible for ^{210}Pb$_{ex}$ over the short period between rainfall events).

We assume that the highest activities of ^{7}Be and ^{210}Pb$_{ex}$ in rainfall occur early in the rain event (initial runoff) and decrease exponentially (Ioannidou and Papastefanou, 2006) (Fig. S5). Pavement-sediment particles transported by initial rainfall-runoff receive the highest amounts of ^{7}Be and ^{210}Pb$_{ex}$ because sediment mass is small relative to rainwater volume. These particles are transported to the stream where they contribute to the radionuclide activities of SS and, to a lesser degree, bed sediment (Fig. 9). This initial runoff of tagged sediment is reflected in elevated ^{7}Be and ^{210}Pb$_{ex}$ activities (Figs. S3A–C) and SSC in the runoff samples (Table S7).

Throughout the runoff period (Fig. 9), pavement sediment continues to be tagged by rain, a process that is cumulative, but activities in pavement sediment are lower than those in runoff sediment for three possible reasons: (1) lower rainfall activities of ^{7}Be and ^{210}Pb$_{ex}$ later in the event, (2) the relatively greater ratio of residual pavement sediment mass to rainfall volume compared to that of suspended sediment mass in runoff to rainfall volume (i.e., runoff water), and (3) dilution of the remaining pavement sediment with soil during the event as soil is eroded and transported to adjacent impervious surfaces. Fallout radionuclide analysis confirms that pavement sediment contains a component of soil. The suspended sediment collected at the Alexander Culvert integrates activities over the storm hydrograph, which includes the higher activities of ^{7}Be and ^{210}Pb$_{ex}$ in the initial runoff and lower activities of ^{7}Be and ^{210}Pb$_{ex}$ from later runoff and from topsoil and bank material (Fig. 9).

The results of this study indicate that the proportion of pavement sediment in suspended sediment in the buried-channel part of the urban watershed is substantially higher than in the open-channel reaches. As a result, concentrations of urban pavement-related contaminants associated with suspended sediment also are likely to be higher in buried channels. The part of an urban watershed that is directly connected to the stream by stormwater drains and buried channels has been termed "effective imperviousness" (Booth and Jackson, 1997), and has been reported to be a better predictor of ecologically relevant geomorphic indicators (Vietz et al., 2014) and bedload yield (Russell et al., 2018) than the percentage of total impervious cover over the watershed. Our results indicate that the better prediction capability may be because "effective imperviousness" better represents areas of potential contaminant transport to the stream than does total impervious area. Delineating the part of an urban watershed that contains buried channels may provide insight into how sediment and contaminants are transported in urban environments.

4. Summary and conclusion

Our results indicate that material washed from impervious surfaces (pavement sediment) is an important contributor to urban stream sediment, especially in areas with large amounts of impervious surface and buried channels. Pavement sediment can be a vector for many common urban contaminants and can be an especially important contributor to receiving streams where networks of buried channels exit into open channels. Activities of ^{7}Be and ^{210}Pb$_{ex}$ in fluvial sediment differ between buried and open channels. Fallout of ^{7}Be and ^{210}Pb$_{ex}$ in rainfall and radionuclide tagging of pavement sediment increases the activities on the sediment, which also contains relic activities from previous events. We hypothesize that the low ratio of sediment mass to rainfall volume in entrained sediment results in higher activities in the runoff sediment than in the pavement sediment, which in turn is—for the same reason—more highly tagged than soils. As runoff particles move through buried channels, activities of ^{7}Be and ^{210}Pb$_{ex}$ remain high. With the exception of material entering buried channels through cracks and breaks, there is limited opportunity for dilution by soils and streambank erosion. Once the suspended sediment moves into the open-channel parts of the watershed, ^{7}Be and ^{210}Pb$_{ex}$ activities are diluted by contributions of lower-activity sediment from stream beds and streambanks. These findings support the hypothesis that sediment from urban impervious surfaces is substantially enriched in ^{210}Pb$_{ex}$ and ^{7}Be from rainfall but not in ^{137}Cs, resulting in a unique radionuclide signature compared to other sediment-source settings. This difference in source activity provides a tool for identifying the sediment contribution to streams from heavily developed urban areas and suggests the need to define source terms by land use in regional stream sediment source and age studies using fallout radionuclide tracers.

Declaration of Competing Interest

The authors declare that they have no known competing financial interests or personal relationships that could have appeared to influence the work reported in this paper.

Acknowledgements

The authors acknowledge assistance in this study from USGS personnel Zachary Grzywacz for field and laboratory assistance, Shannon Jackson for GIS support, and Jeff Klein for construction of the passive samplers. We would like thank Dr. Joel Moore, Towson University, for suggestions and review, and three anonymous reviewers for helpful comments, all which greatly improved this paper. Data generated during this study are available as a USGS data release (Clifton et al., 2019).

This research was funded by the U.S. Geological Survey National Water Quality Program. Funding for operation and maintenance of USGS stream gage 01589312 and the rain gage located at that site, as well as time of C. Welty, A.J. Miller, and J.T. Kemper was provided in part by NSFGrants # EAR-1427150 and DEB-1637661; NSF cooperative agreement #CBET-1444758; and Chesapeake Bay Trust Grant #12507.

Any use of trade, firm, or product names is for descriptive purposes only and does not imply endorsement by the U.S. Government.

Appendix A. Supplementary data

Supplementary data to this article can be found online at https://doi.org/10.1016/j.jhydrol.2020.124855.

References

Ali, H., Choi, J.-H., 2019. A review of underground pipeline leakage and sinkhole monitoring methods based on wireless sensor networking. Sustainability 11 (15), 4007.

Bain, D.J., Yesilonis, I.D., Pouyat, R.V., 2012. Metal concentrations in urban riparian sediments along an urbanization gradient. Biogeochemistry 107, 67–79.

Barnes, M.L., Welty, C., Miller, A.J., 2018. Impacts of development pattern on urban groundwater flow regime. Water Resour. Res. 54 (8), 5198–5212.

Benmansour, M., Mabit, L., Owens, P.N., Tarjan, S., Walling, D.E., 2014. The use of excess ^{210}Pb (^{210}Pb$_{ex}$) as a soil and sediment tracer measurements. In: Guidelines for Using Fallout Radionuclides to Assess Erosion and Effectiveness of Soil Conservation Strategies, IAEA-TECDOC-1741. IAEA, Vienna p, pp. 3–26.

Boonyatumanond, R., Murakami, M., Wattayakorn, G., Togo, A., Takada, H., 2007. Sources of polycyclic aromatic hydrocarbons (PAHs) in street dust in a tropical Asian mega-city, Bangkok, Thailand. Sci. Total Environ. 384, 420–432.

Booth, D.B., 1990. Stream-channel incision following drainage-basin urbanization. Water Resour. Res. 26, 407–417. https://doi.org/10.1111/j.1752-1688.1990.tb01380.x.

Booth, D.B., 1991. Urbanization and the natural drainage system-impacts, solutions, and prognoses. Northwest Environ. J. 7, 93–118.

Booth, D.B., Jackson, C.R., 1997. Urbanization of aquatic systems: degradation thresholds, stormwater detection, and the limits of mitigation. J. Am. Water Resour. Assoc. 33, 1077–1090.

Broadhead, A.T., Lerner, D.N., 2013. www.daylighting.org.uk: case study website supporting research into daylighting urban rivers. Hydrol. Processes 27 (12), 1840–1842.

Broadhead, A.T., Horn, R., Lerner, D., 2015. Finding lost streams and springs captured in combined sewers: a multiple lines of evidence approach. Water Environ. J. 29, 288–297.

Caillet, S., Arparagaus, P., Monna, F., Dominik, J., 2001. Factors controlling ^{7}Be and ^{210}Pb atmospheric deposition as revealed by sampling individual rain events in the region of Geneva. J. Environ. Radioact. 53, 241–256.

Callender, E., Rice, K.C., 2000. The urban environmental gradient: anthropogenic influences on the spatial and temporal distributions of lead and zinc in sediments. Environ. Sci. Technol. 34 (2), 232–238.

Cannon, W.F., Horton, J.D., 2009. Soil geochemical signature of urbanization and industrialization – Chicago, Illinois, USA. Appl. Geochem. 24, 1590–1601.

Cashman, M.J., Gellis, A.C.. Gorman Sanisaca, L., Noe, G., Cogliandro, V., Baker., A., 2018. Bank-derived sediment dominates in a suburban Chesapeake Bay watershed, Upper Difficult Run, Virginia, USA. River Research and Applications, published on line, DOI: 10.1002/rra.3325. https://onlinelibrary.wiley.com/doi/epdf/10.1002/rra.3325=.

Clifton, Z.J., Gellis, A.C., Malen, J.M., Grzywacz, Z.T., Fuller C.C., and Van Metre P.C., 2019. Urban sediment and fallout radionuclide input characteristics of Dead Run watershed in Catonsville, Maryland for 2017-2018 (Version 1.1, January, 2020) : U.S. Geological Survey data release, https://doi.org/10.5066/P9K86P4Q.

Collins, A.L., Zhang, Y., McChesney, D., Walling, D.E., Haley, S.M., Smith, P., 2011. Sediment source tracing in a lowland agricultural catchment in southern England using a modified procedure combining statistical analysis and numerical modelling. Sci. Tot. Environ. 414, 301–317.

Conaway, C.H., Storlazzi, C.D., Draut, A.E., Swarzenski, P.W., 2013. Short-term variability of ^{7}Be atmospheric deposition and watershed response in a Pacific coastal stream, Monterey Bay, California, USA. J. Environ. Radioact. 120, 94e103.

Crowley, W.P., 1976. The geology of the crystalline rocks near Baltimore and its bearing on the evolution of the eastern Maryland Piedmont: Maryland Geological Survey. Report of Investigations 27, 40 p.

Devereux, O.H., Prestegaard, K.L., Needelman, B.A., Gellis, A.C., 2010. Suspended-sediment sources in an urban watershed, Northeast Branch Anacostia River, Maryland. Hydrol. Process. 24, 1391–1403. https://doi.org/10.1002/hyp.7604.

Dominik, J., Burrus, D., Vernet, J.P., 1987. Transport of the environmental radionuclides in an alpine watershed. Earth Planetary Sci. Lett. 84, 165–180. https://doi.org/10.1016/0012-821X(87)90083-5.

Duncan, J.M., Welty, C., Kemper, J.T., Groffman, P.M., Band, L.E., 2017. Dynamics of nitrate concentration-discharge patterns in an urban watershed. Water Resour. Res. 53, 7349–7365. https://doi.org/10.1002/2017WR020500.

Eckley, C.S., Branfireun, B., 2008. Gaseous mercury emissions from urban surfaces: controls and spatiotemporal trends. Appl. Geochem. 23, 369–383.

Ellis, J.B., 2001. Sewer Infiltration/Exfiltration and Interactions with Sewer Flows and Groundwater Quality," Interurba II, Lisbon, 19-22 February 2001, p. 311-319.

Elmore, A.J., Kaushal, S.S., 2008. Disappearing headwaters: patterns of stream burial due to urbanization. Front. Ecol. Environ. 6, 308–312.

Evrard, O., Némery, J., Gratiot, N., Duvert, C., Ayrault, S., Lefèvre, I., Poulenard, J., Prat, C., Bonté, P., Esteves, M., 2010. Sediment dynamics during the rainy season in tropical highland catchments of central Mexico using fallout radionuclides. Geomorphology 124, 42–54.

Fergusson, J.E., Ryan, D.E., 1984. The elemental composition of road dust from large and small urban areas related to city type, source and particle size. Sci. Total Environ. 34, 101–116.

Froger, C., Ayrault, S., Evrard, O., Monvoisin, G., Bordier, L., Lefèvre, I., Quantin, C., 2018.Tracing the sources of suspended sediment and particle-bound trace metal elements in an urban catchment coupling elemental and isotopic geochemistry, and FRNs: Environmental Science and Pollution Research, published online, https://doi.org/10.1007/s11356-018-2892-3.

Fuller, C.C., van Green, A., Baskaran, M., Anima, R., 1999. Sediment chronology in San Francisco Bay, California defined by ^{210}Pb, ^{234}Th, ^{137}Cs, and ^{239,240}Pu. Mar. Chem 64, 7–27.

Gellis, A.C., Fuller, C.C., Van Metre, P.C., 2017b. Sources and ages of fine-grained sediment to streams using FRNs in the Midwestern United States. J. Environ. Manage. 194 (1), 73–85.

Gellis, A.C., Gorman Sanisaca, L., 2018. Sediment fingerprinting to delineate sources of sediment in the agricultural and forested Smith Creek watershed, Virginia, USA. J. Am. Water Resour. Assoc. 54 (6), 1197–1221.

Gellis, A.C., Myers, M.K., Noe, G.B., Hupp, C.R., Schenk, E.R., Myers, L., 2017a. Storms, channel changes, and a sediment budget for an urban-suburban stream, Difficult Run, Virginia, USA. Geomorphology 278, 128–148.

Gourdin, E., Evrard, O., Huon, S., Reyss, J.L., Ribolzi, O., Bariac, T., Sengtaheuanghoung, O., Ayrault, S., 2014. Spatial and temporal variability of ^{7}Be and ^{210}Pb wet deposition during four successive monsoon storms in a catchment of northern Laos. J. Environ. Radioact. 136, 195–205.

Hancock, G.J., Wilkinson, S.N., Hawdon, A.A., Keen, R.J., 2014. Use of fallout tracers ^{7}Be, ^{210}Pb and ^{137}Cs to distinguish the form of sub-surface soil erosion delivering sediment to rivers in large catchments. Hydrol. Process. 28, 3855–3874.

Hatcher, C.L., Filippelli, G.M., 2010. Mercury cycling in an urbanized watershed: the influence of wind distribution and regional subwatershed geometry in Central Indiana, USA. Water Air Soil Pollut 219, 251–261.

He, Q., Walling, D.E., 1996. Interpreting particle size effects in the adsorption of ^{137}Cs and unsupported ^{210}Pb by mineral soils and sediments. J. Environ. Radioact. 30, 117–137.
Heathcoate, I.W., 2009. Integrated Watershed Management: Principles and Practice. 2009. 2nd Edition. John Wiley & Sons, Inc., New Jersey.
Huh, C.A., Su, C.C., 2004. Distribution of FRNs (^{7}Be, ^{137}Cs, ^{210}Pb and ^{239,240}Pu) in soils of Taiwan. J. Environ. Radioact. 77, 87–100.
Huon, S., Evrard, O., Gourdin, E., Lefévre, I., Bariac, T., Reyss, J.L., des Tureaux, T.H., Sengtaheuanghoung, O., Ayrault, S., Ribolzi, O., 2017. Suspended sediment source and propagation during monsoon events across nested sub-catchments with contrasted land uses in Laos. J. Hydrol. Reg. Stud. 9, 69–84.
Ioannidou, A., Papastefanou, C., 2006. Precipitation scavenging of Be-7 and (CS)-C-137 radionuclides in air. J. Environ. Radioact. 85 (1), 121–136.
Jorgenson, B.C., Young, T.M., 2010. Formulation effects and the off-target transport of pyrethroid insecticides from urban hard surfaces. Environ. Sci. Tech. 44, 4951–4957.
Kaste, J.M., Norton, S.A., Hess, C.T., 2002. Environmental Chemistry of Beryllium-7. Mineralogical Society of America, Special Volume 50, 271-289.
Karwan, D.L., Siegert, C.M., Levia, D.F., Pizzuto, J., Marquard, J., Aalto, R., Aufdenkampe, A.K., 2016. Beryllium-7 wet deposition variation with storm height, synoptic classification, and tree canopy state in the mid-Atlantic USA. Hydrol. Process. 30, 75–89.
Kemper, J.T., Miller, A.J., Welty, C.W., 2019. Spatial and temporal patterns of suspended sediment transport in nested urban watersheds. Geomorphology 336, 95–106.
Leopold, L.B., 1968. Hydrology for Urban Land Planning - A Guidebook on the Hydrologic Effects of Urban Land Use. U.S Geol. Survey Circ. 55, 18.
Loganathan, P., Vigneswaran, S., Kandasamy, J., 2013. Road-deposited sediment pollutants: a critical review of their characteristics, source apportionment, and management Crit. Rev. Environ. Sci. Technol. 43 (13), 1315–1348.
Mabit, L., Benmansour, M., Abril, J.M., Walling, D.E., Meusburger, K., Iurian, A.R., Bernard, C., Tarján, S., Owens, P.N., Blake, W.H., Alewell, C., 2014. Fallout ^{210}Pb as a soil and sediment tracer in catchment sediment budget investigations - A review. Earth Sci Rev 138, 335–351.
Mahler, B.J., Van Metre, P.C., Bashara, T.J., Wilson, J.T., Johns, D.A., 2005. Parking lot sealcoat: An unrecognized source of urban PAHs. Environ. Sci. Technol. 39 (15), 5560–5566.
Matisoff, G., Wilson, C.G., Whiting, P.J., 2005. The ^{7}Be/^{210}Pb$_{xs}$ ratio as an indicator of suspended sediment age or fraction new sediment in suspension. Earth Surf. Process. Landforms 30, 1191–1201.
McNeary, D., Baskaran, M., 2003. Depositional characteristics of ^{7}Be and ^{210}Pb in southeastern Michigan. J. Geophys. Res. 108 (D7), 4210. https://doi.org/10.1029/2002JD003021.
Motha, J.A., Walbrink, P.J., Hairsine, P.B., Grayson, R.B., 2002. Tracer properties of eroded sediment and source material. Hydrol Process 16, 1983–2000.
Nakano, Y., Inoue, M., Komura, K., 2008. Simple coprecipitation method combined with low background γ-spectrometry: determination of ^{7}Be, ^{137}Cs, ^{210}Pb, and radium and thorium isotopes in small volume coastal water samples. J. Oceanogr. 64 (5), 713–717.
Napieralski, J.A., Carvalhaes, T., 2016. Urban stream deserts: mapping a legacy of urbanization in the United States. Appl. Geogr. 67, 128–129.
Navas, A., Gaspar, L., López-Vicente, M., Machín, J., 2011. Spatial distribution of natural and artificial radionuclides at the catchment scale (South Central Pyrenees). Radiat. Meas. 46 (2), 261–269.
Olley, J., Brooks, A., Spencer, J., Pietsch, T., Borombovits, D., 2013a. Subsoil erosion dominates the supply of fine sediment to rivers draining into Princess Charlotte Bay, Australia. J. Environ. Radioact. 124, 121–129.
Olley, J., Burton, J., Smolders, K., Pantus, F., Pietsch, T., 2013b. The application of fallout radionuclides to determine the dominant erosion process in water supply catchments of subtropical south-east Queensland, Australia. Hydrol. Process. 27, 885–895.
Paul, M.J., Meyer, J.L., 2001. Streams in the Urban Landscape. Annu. Rev. Ecol. Syst. 32, 333–365.
Phillips, J.M., Russell, M.A., Walling, D.E., 2000. Time-integrated sampling of fluvial suspended sediment: a simple methodology for small catchments. Hydrol. Process. 14, 2589–2602.
Porto, P., Walling, D.E., Callegari., G., La Spada, C., 2010. Exploring the relationship between sediment and FRN output for two small Calabrian catchments. In: Banasik (Ed.), Sediment dynamics for a changing future, vol. 273. IAHS PRESS, Wallingford (GBR), pp. 163–171.
Ritchie, J.C., McHenry, J.R., 1990. Application of radioactive fallout cesium-137 for measuring soil erosion and sediment accumulation rates and patterns: a review. J. Environ. Quality 19, 215–233.
Russell, K.L., Vietz, G.F., Fletcher, T.D., 2019. A suburban sediment budget: Coarse-grained sediment flux through hillslopes, stormwater systems and streams. Earth Surf. Proc. Land. 44, 2600–2614.
Russell, K.L., Vietz, G.F., Fletcher, T.D., 2018. Urban catchment runoff increases bedload sediment yield and particle size in stream channels. Anthropocene 23, 53–66.
Sansalone, J.J., Cristina, C.M., 2004. First flush concepts for suspended and dissolved solids in small impervious watersheds. J. Environ. Eng. 130 (11), 1301–1314.
Sartor, J., Boyd, G.B., Agardy, F.J., 1974. Water pollution aspects of street surface contaminants. J. Water Pollut. Contr. Federation 46 (3), 458–465.
Sato, M., Kuwano, R., 2015. Influence of location of subsurface structures on development of underground cavities induced by internal erosion. Soils Found. 55, 829–840.
Schuller, P., Walling, D.E., Iroumé, A., Quilodrán, C., Castillo, A., Navas, A., 2013. Using ^{137}Cs and ^{210}Pb$_{ex}$ and other sediment source fingerprints to document suspended sediment sources in small forested catchments in south-central Chile. J Environ Rad 124, 147–159.
Selbig, W.R., Bannerman, R.T., 2007. Evaluation of street sweeping as a stormwater-quality-management tool in three residential basins in Madison, Wisconsin: U.S. Geological Survey Scientific Investigations Report 2007–5156, 103 p.
Slimane, A.B., Raclot, D., Evrard, O., Sanaa, M., Lefevre, I., Bissonnais, Y., 2016. Relative contribution of rill/interrill and gully/channel erosion to small reservoir siltation in Mediterranean environments. Land Degrad. Dev. 27 (3), 785–797.
Southworth, G., Mathews, T., Greeley, M., Peterson, M., Brooks, S., Ketelle, D., 2013. Sources of mercury in a contaminated stream—implications for the timescale of recovery. Environ. Toxicol. Chem. 32, 764–772.
Tang, Y., Zhu, D.Z., and Chan, D.H., 2018, Modeling soil loss by water infiltration through sewer pipe defects. Kamojjala, S., ed., Hydraulics and Waterways, Water Distribution Systems Analysis, and Smart Water, World Environmental and Water Resources Congress 2018, 254-262.
Taylor, K.G., Owens, P.N., 2009. Sediments in urban river basins: a review of sediment-contaminant dynamics in an environmental system conditioned by human activities. J Soils Sediments 9, 281–303.
Taylor, A., Blake, W.H., Keith-Roach, M.J., 2014. Estimating Be-7 association with soil particle size fractions for erosion and deposition modelling. J. Soils Sediments 14, 1886–1893.
Taylor, A., Blake, W.H., Couldrick, L., Keith-Roach, M.J., 2012. Sorption behaviour of beryllium-7 and implications for its use as a sediment tracer. Geoderma 187–188, 16–23.
Teramage, M.T., Onda, Y., Kato, H., Wakiyama, Y., Mizugaki, S., Hiramatsu, S., 2013. The relationship of soil organic carbon to ^{210}Pb$_{ex}$ and ^{137}Cs during surface soil erosion in a hillslope forested environment. Geoderma 192, 59–67.
Thapalia, A., Borrok, D.M., Van Metre, P.C., Musgrove, M., Landa, E.R., 2010. Zn and Cu isotopes as tracers of anthropogenic contamination in a sediment core from an urban lake. Environ. Sci. Technol. 44, 1544–1550.
Todd, J.F., Wong, G.T.F., Olsen, C.R., Larsen, I.L., 1989. Atmospheric depositional characteristics of beryllium 7 and lead 210 along the southeastern Virginia Coast. J. Geophys. Res. 94, 11106–11116.
U.S. Geological Survey, 2019, USGS 01589312 Dead Run near Catonsville, MD in USGS water data for the Nation: U.S. Geological Survey National Water Information System database, accessed December 21, 2018, at https://doi.org/10.5066/F7P55KJN. [Site information directly accessible at https://waterdata.usgs.gov/nwis/dv?referred_module=sw&site_no=01589312.].
Van Metre, P.C., Mahler, B.J., 2003. The contribution of particles washed from rooftops to contaminant loading to urban streams. Chemosphere 52, 1727–1741.
Van Metre, P.C., Wilson, J.T., Fuller, C.C., Callender, E., Mahler, B.J., 2004. Collection, analysis, and age-dating of sediment cores from 56 U.S. lakes and reservoirs sampled by the U.S. Geological Survey, 1992–2001: U.S. Geological Survey Scientific Investigations Report 2004–5184, 180 p.
Vietz, G.J., Sammonds, M.J., Walsh, C.J., Fletcher, T.D., Rutherfurd, I.D., Stewardson, M.J., 2014. Ecologically relevant geomorphic attributes of streams are impaired by even low levels of watershed effective imperviousness. Geomorphology 206, 67–78.
Wallbrink, P.J., Murray, A.S., 1996. Determining soil loss using the inventory ratio of excess lead-210 to cesium-137. Soil Sci. Soc. Am. J. 60, 1201–1208.
Wallbrink, P., Olley, J.M., Hancock, G., 2002. Estimating residence times of fine sediment in river channels using fallout ^{210}Pb. In: The Structure, Function and Management Implications of Fluvial Sedimentary Systems, Fiona J. Dyer, Martin C. Thoms, Jon M. Olley, eds., Proceedings of an international symposium held at Alice Springs, Australia. September 2002, IAHS Publ. no. 276, p. 425-432.
Walling, D.E., 2005. Tracing suspended sediment sources in catchments and river systems. Sci. Total Environ. 344 (1–3), 159–184.
Walsh, C.J., Roy, A.H., Feminella, J.W., Cottingham, P.D., Groffman, P.M., Morgan, R.P., 2005. The urban stream syndrome: current knowledge and the search for a cure. J. North Am. Benthol. Soc. 24 (3), 706–723.
Waschbush, R.J., 2003. Data and methods of a 1999-2000 road sweeping study on an urban freeway in Milwaukee County, Wisconsin. U.S. Geological Survey Open-File Report 03-93, 41p.
Watts, A.W., Ballestero, T.P., Roseen, R.M., Houle, J.P., 2010. Polycyclic aromatic hydrocarbons in stormwater runoff from sealcoated pavements. Environ. Sci. Technol. 44 (23), 8849–8854.
Wolman, M.G., 1967. A cycle of sedimentation and erosion in urban river channels. Geogr. Ann. Ser. A Phys. Geogr. 49, 385–395.